IPPJ-AM-60

THEORY OF THRESHOLD ENERGY OF ION-INDUCED DESORPTION BY A FEW-COLLISION MODEL

Y. YAMAMURA, J. BOHDANSKY
AND E. TAGLAUER

INSTITUTE OF PLASMA PHYSICS
NAGOYA UNIVERSITY

NAGOYA, JAPAN

IPPJ-AM-60

THEORY OF THRESHOLD ENERGY OF ION-INDUCED DESORPTION BY A FEW-COLLISION MODEL

Y. Yamamura[1], J. Bohdansky[2] and E. Taglauer[2]

Institute of Plasma Physics, Nagoya University
Chikusa-ku, Nagoya 464-01, Japan

April 1988

Permanent address:
1) Okayama University of Science, Ridai-cho, Okayama 700, Japan
2) Max-Plank-Institut für Plasmaphysik, Euratom Association
D-8046, Garching bei München, Fed. Rep. of Germany

Abstract

Assuming a few-collision sequence near the surface for the near-threshold ion-induced desorption, analytic formulae for the threshold energies of the ion-induced desorption are derived for possible combinations of the projectile, the substrate and the adsorbate under the condition that the adsorbate atoms are isolated from each other. The obtained formulae include explicitly the angle of incidence. The ion-induced desorption thresholds are found to depend strongly on the combination of the projectile, the substrate atom, and the adsorbate atom.

The threshold mechanism corresponds tc the minimum energy-loss process. The minimum energy-loss condition says that the particle with the smallest mass among the projectile, the substrate atom and the adsorbate atom should move in solids.

It is found that the atomic mass of the projectile is larger than that of the substrate atom, the desorption threshold is a decreasing function of the angle of incidence. On the other hand, when the atomic mass of the projectile is less than those of the substrate atom and the adsorbate atom or when the atomic mass of the adsorbate atom is less than those of the substrate atom and the projectile, the desorption thresholds are not sensitive to the angle of incidence.

I . INTRODUCTION

The surface of the wall material in a fusion reactor is usually covered with adsorbate atoms such as H, D, S, etc. Due to bombardment of ion, electron and photon, these adsorbed atoms are released into the plasma boundary. Thus, surface layers are a significant source of both plasma particles and impurities and therefore play an important role for hydrogen recycling and impurity flux. Yields of the ion-induced desorption are much higher by a factor of two or three than those of electron-induced and photon-induced desorptions. Therefore, the concern of this paper is the ion-induced desorption.

The temperature of the edge plasma is very low and usually less than 100 eV, meanwhile the binding energy of adsorbed atom is of the order of 0.5 eV for physisorption and is of the order of several electron volts for chemisorption. Therefore it is very important to know the threshold energy of the ion-induced desorption.

About ten years ago Liu et al. investigated theoretically and experimentally the threshold energy for the desorption of hydrocarbons from silver under Ar^+ ion impact[1]. Using a single collision model, they derived a simple formula for the threshold energy, but their model did not take into account the effect of the surface binding energy and the collision between the adsorbate atom and the substrate surface explicitly.

Up to now there is no theory on the the threshold energy of the ion-induced desorption which can be applied to any combination of a projectile, a substrate atom, and an adsorbate atom. Employing the binary collision approximation and a-few-collision model[2], in this paper, a simple analytic formula for the threshold energy of the ion-induced desorption will be derived under the assumption that the adsorbed atoms are completely isolated from each other.

II . A FEW-COLLISION MODEL AND THEORY OF DESORPTION THRESHOLDS

Recent computer simulations on the low-energy sputtering indicate that the collision sequences leading to the ejection of target atoms are very short for the near-threshold sputtering and that the collision events take place at topmost layer or the second layer [3,4]. It is quite reasonable to assume that this situation would be similar to the ion induced-desorption process in the near-threshold energy region.

In the case that adsorbed atoms are completely isolated from each other, three different mechanisms can contribute to the ion-induced desorption process[5], i.e., the direct knockoff contribution (Mechanism 1), the reflected-ion contribution (Mechanism 2), and the sputtered-atom contribution (Mechanism 3). Schematic representations of these three mechanisms are given in Fig. 1, where Mechanism 3 is further divided into

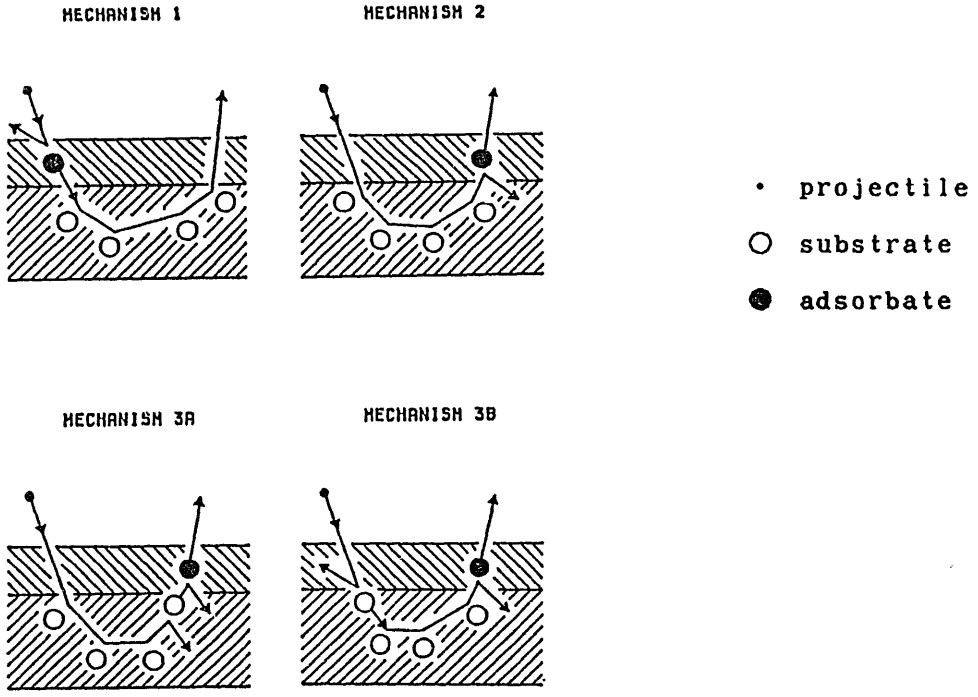

Fig. 1 Schematic representations of ion-induced desorption mechanism, where the adsorbate atom is assumed to be completely isolated.

two patterns, i.e., Mechanism 3A and Mechanism 3B. In the case of Mechanism 3A the projectile moves inside the substrate, while the substrate atom moves inside the substrate in the case of Mechanism 3B.

The most important factor of determining the threshold energy is the binding force between the adsorbed atom and substrate atoms. Physisorption is due to van der Waals force which is a long-range interaction. Therefore the planar potential is very reasonable as the surface barrier between an outgoing adsorbed atom and substrate atoms. On the other hand, chemisorption is due to exchange or sharing of electrons between an adsorbate atom and a substrate atom, since the speeds of outgoing adsorbate atoms due to the low-energy ion bombardment are very slow as compared with those of the valence electrons. Then,in this paper, we will employ the planar potential as the surface barrier for the ion-induced desorption.

2.1 Mechanism 1

In the case of Mechanism 1 an incoming projectile hits an adsorbate, and the adsorbate is reflected from the substrate surface either directly or after several collisions. Let E_0 be the incident energy of the projectile, and θ_0 be the angle of incidence which is measured from the surface normal (see Fig. 2).

If the atomic configuration of the solid is fixed, the scattering angles of subsequent collisions are a function of the impact parameter of the first collision between the projectile and the adsorbate atoms. However, it is reasonable that for the threshold desorption in an amorphous target any atomic configuration is allowed [2]. This assumption means that each scattering angle of the successive collisions is an independent variable [2].

Since the minimum energy-loss process is the equal-scattering angle one in the incident plane, the scattering angles of the successive (m + 2) collisions after the first collision are assumed to be equal. Then, the

energies and total scattering angles are given as

$$E_1 = E_0 \gamma_{13} \sin^2 \frac{\phi_1}{2} , \tag{1}$$

$$E_{m+3} = E_1 (1 - \gamma_{32} \sin^2 \frac{\beta_m}{2})^{m+2} , \tag{2}$$

$$\theta_1 = \theta_0 + (\pi - \phi_1) / 2 , \tag{3}$$

$$\theta_{m+3} = \theta_1 + (m + 2) \alpha_m , \tag{4}$$

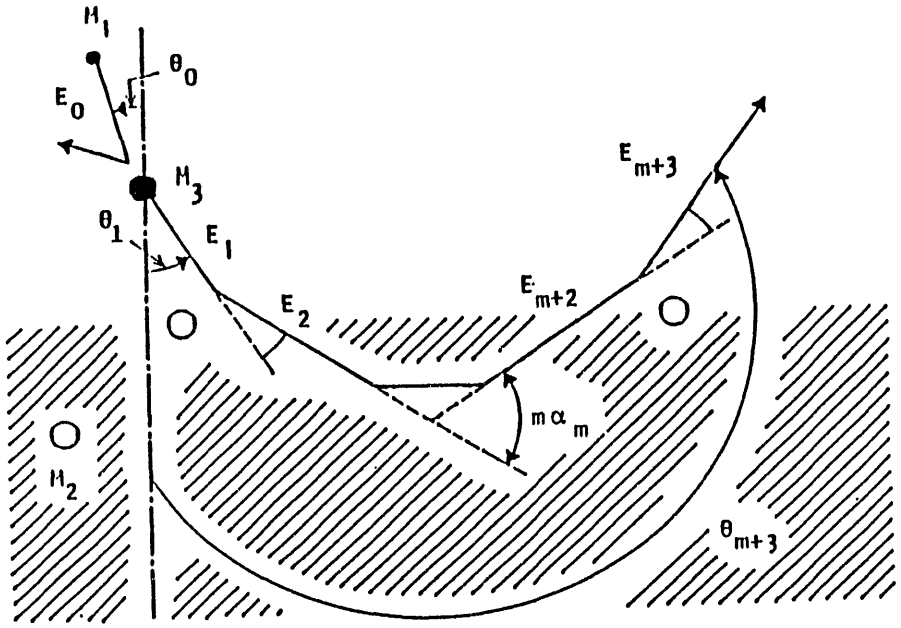

Fig. 2 The schematic representation of ion-induced desorption process due to Mechanism 1

where ϕ_1 is the scattering angle in the center-of-mass (CM) system at the first collision, β_m is the CM scattering angle of the equal-angle scattering process inside the solid, α_m is the scattering angle in the laboratory (L) system, and θ_j is the total scattering after the j-th collision which is measured from the surface normal. The energy transfer factor γ_{ij} is given as

$$\gamma_{ij} = \frac{4M_iM_j}{(M_i + M_j)^2} , \tag{5}$$

where M_1, M_2 and M_3 are the atomic masses of projectile, the substrate atom, and the adsorbate atom, respectively.

Since we assume the planar potential as the surface barrier, the vertical component E^I_+ of the energy of the outgoing adsorbate atom is given as follows:

$$E^I_+ = E_0\gamma_{13}\sin^2\frac{\phi_1}{2}\left(1 - \gamma_{32}\sin^2\frac{\beta_m}{2}\right)^{m+2}$$

$$\times \sin^2\left(\theta_0 - \frac{\phi_1}{2} + (m+2)\alpha_m\right) . \tag{6}$$

Since we assume random configuration of substrate atoms for the near threshold desorption, the scattering angle ϕ_1 and α_m are independent variables. The threshold energy of this mechanism corresponds to the maximum value of E^I_+ which can be obtained by differentiating E^I_+ step by step with respect to ϕ_1 and α_m.

From the condition of $\delta E^I_+/\delta\alpha_m = 0$ we have

$$\theta_0 + \frac{\pi - \phi_1}{2} + (m+2)\alpha_m + \theta = \pi , \tag{7}$$

where

$$\theta = \arccos(1 - \mu_{32}^2 \sin^2\alpha_m)^{1/2} \tag{8}$$

with the definition of $\mu_{32} = M_3 / M_2$.

Using the maximum condition of Eq. (7) the vertical component E^I_+ can be rewritten in the form

$$E^I_+ = E_0 \gamma_{13} \sin^2 \frac{\phi_1}{2} \times \left[\frac{(1 - \mu_{32}^2 \sin^2\alpha_m)^{1/2} + \mu_{32}\cos\alpha_m}{1 + \mu_{32}} \right]^{2m+4} (1 - \mu_{32}^2 \sin^2\alpha_m). \tag{9}$$

The vertical component E^I_+ of Eq. (9) is a function of ϕ_1, and the maximum condition of $\delta E^I_+ / \delta \phi_1 = 0$ yields

$$\theta = \frac{\pi - \phi_1}{2} . \tag{10}$$

Finally we have the expression of the maximum vertical component E^I_+, i.e.,

$$E^I_+ = E_0 \gamma_{13} \cos^4\theta \left[\frac{\cos\theta + (\mu_{32}^2 - \cos^2\theta)^{1/2}}{1 + \mu_{32}} \right]^{2m+4} \tag{11}$$

where θ is the solution of the following transcendental equation:

$$2\theta + (m + 2)\arccos \frac{(\mu_{32}^2 - \sin^2\theta)^{1/2}}{\mu_{32}} = \pi - \theta_0. \tag{12}$$

When the maximum vertical component E^I_+ is equal to the binding energy E_B, the incident energy E_0 corresponds to threshold energy E^I_{th} of Mechanism 1, i.e.,

$$E^I_{th} = \frac{E_B}{\gamma_{13}} \frac{1}{\cos^4\theta} \left(\frac{1 + \mu_{32}}{\cos\theta + (\mu_{32}^2 - \sin^2\theta)^{1/2}} \right)^{2m+4} . \quad (13)$$

Now, let us discuss the condition of the minimum energy-loss process. The recoil angle of the first collision is equal to the supplementary angle θ of the deflection angle of the outgoing adsorbate due to the surface barrier. The angle θ is equal to the scattering angle in the L system when the projectile (adsorbate)is at rest and the target (substrate) atom is moving, and so there is a very simple relation between α_m and θ, i.e., $\alpha_m + \theta = \beta_m$. This relation means that the transcendental equation (12) can be solved analytically only for m = 0, where m = 0 corresponds to the three-collision-desorption process.

Unfortunately, the transcendental equation (12) with arbitrary m cannot be solved analytically. The following approximate solution is very useful in the whole region of μ_{32}:

$$\theta \fallingdotseq \mu_{32} \sin \frac{\pi - \theta_0}{m + 2 + 2\mu_{32}}$$

$$\fallingdotseq \frac{\pi - \theta_0}{m + 2 + 2\mu_{32}} \mu_{32} . \quad (14)$$

The comparison between the exact solutions and the approximate values calculated from Eq.(14) is shown in Fig. 3 for m = 2. The agreement is very good in the whole region of the mass ratio μ_{32}, especially for large angles of incidence. The corresponding approximate formula for the

threshold energy is given as

$$\tilde{E}^{I}_{th} = \frac{E_B}{\gamma_{13}} \frac{1}{\cos^2(\tau_{32,m}\,\mu_{32})} \times \left[\frac{1+\mu_{32}}{\cos(\tau_{32,m}\,\mu_{32}) + \mu_{32}\cos(\tau_{32,m})} \right]^{2m+4}, \tag{15}$$

where

$$\tau_{32,m} = \frac{\pi - \theta_0}{m + 2 + 2\mu_{32}}. \tag{16}$$

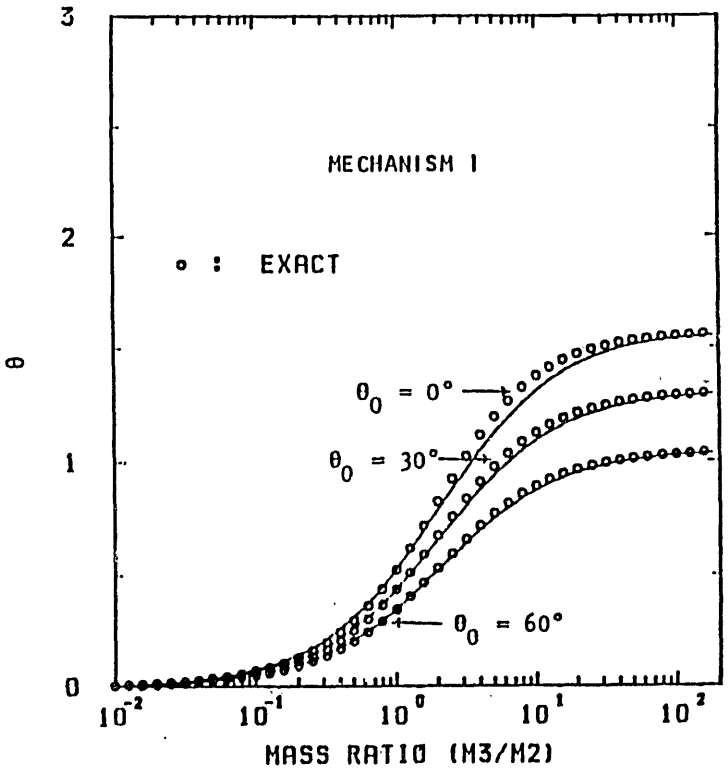

Fig. 3 Comparison of the exact solutions with the approximate solutions which are calculated from Eq. (14). The circular marks mean the exact solution of Eq. (12), and the solid lines correspond to approximate solutions.

The collision number m of Eq. (13) means the number of successive col-

lisions in the substrate which does not include the collisions with substrate atoms at the topmost layer. From the theoretical point of view it is very difficult to determine this collision number m.

In Fig. 4 the m-dependences of threshold energies of Mechanism 1 are shown as a function of the mass ratio μ_{32}, where the approximate threshold energies calculated from Eq. (15) are also drawn in broken lines. As the mass ratio becomes large, threshold energies depend strongly on the mass ratio and the collision number, because the energy loss due to one collision becomes large. The present approximate formula is excellent for $\mu_{32} < 1$.

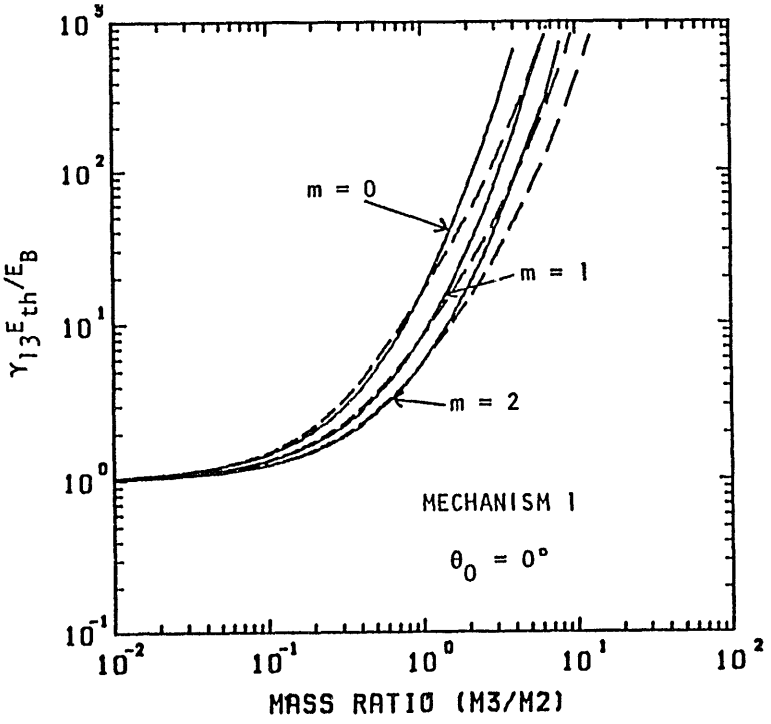

Fig. 4 Comparison of the exact threshold energies E^I_{th} (Eq.(13)) with the approximate $\tilde{E}^I_{th}$ which are calculated from Eq. (15), where the angle of incidence is normal, and m is the collision number inside the substrate material. The solid lines and the broken lines correspond to E^I_{th} and $\tilde{E}^I_{th}$, respectively.

2.2 Mechanism 2

In the case of Mechanism 2 a projectile penetrates furtherinto the substrate target after collision with the substrate atom, and it is reflected at some depth in the substrate. On its way out the reflected projectile knocks off the adsorbed atom on the topmost layer.

The schematic representation of Mechanism 2 is drawn in Fig. 5. After the first collision the projectile with energy E_1 is assumed to make (m+1) equal-angle scatterings with substrate atoms. The vertical component E^{II}_{+} of the energy E_{m+3} of the knocked off adsorbate is given as

$$E^{II}_{+} = E_0 \gamma_{13}(1 - \gamma_{12}\sin^2\frac{\phi_1}{2})(1 - \gamma_{12}\sin^2\frac{\beta_m}{2})^{m+1}\sin^2\frac{\phi_2}{2}$$

$$\times \sin^2(\theta_0 + \theta_a + (m+1)\alpha_m - \frac{\phi_2}{2}), \qquad (17)$$

where ϕ_2 is the CM scattering angle at the (m + 3)th collision of the projectile with the adsorbate atom, and θ_a is the scattering angle in the L system at the first collision which is represented in terms of the CM scattering ϕ_1, i.e.,

$$\theta_a = \arctan\frac{\sin\phi_1}{\mu_{12} + \cos\phi_1} . \qquad (18)$$

Mechanism 2 of the ion-induced desorption is very similar to Mechanism 2C of the sputtering threshold in Ref. 2. Then we can easily know the maximum condition of the vertical component E^{II}_{+} of Eq. (17). The maximum conditions are the following:

1) The scattering angle θ_a is equal to the scattering angle α_m which is the scattering angle in the L system during the successive (m + 1) equal-angle scattering process.

2) The recoil angle is equal to the angle θ_b which is the scattering angle in the L system when the projectile is at rest and the substrate atom is moving, i.e.,

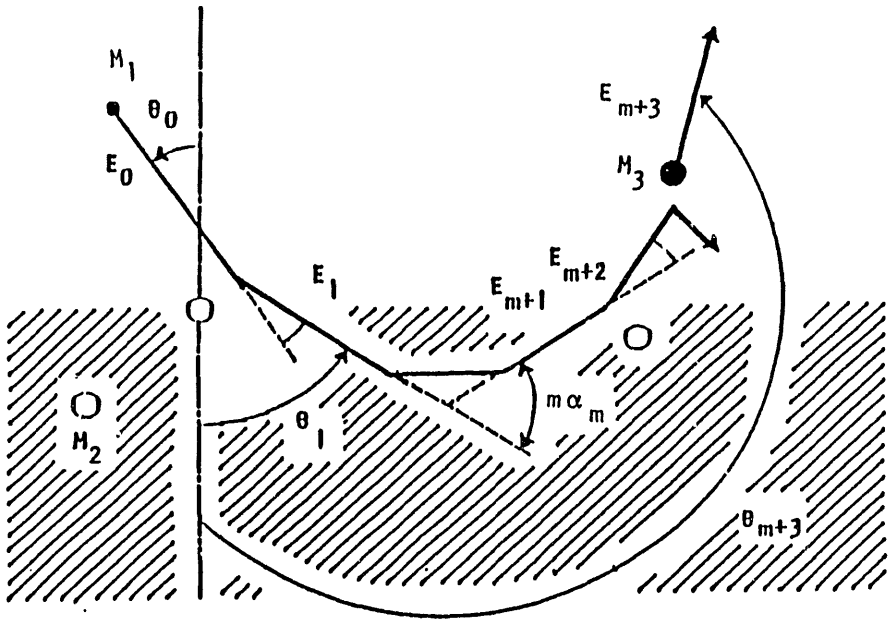

Fig. 5 The schematic representation of ion-induced desorption of Mechanism 2

$$\theta_b = \arctan \frac{\mu_{12} \sin\phi_1}{1 + \mu_{12} \cos\phi_1} . \qquad (19)$$

Therefore there is a simple relation of $\theta_a + \theta_b = \phi_1$.

3) The supplementary angle of the deflection angle of the outgoing adsorbate is equal to the angle θ_b.

Using the above-mentioned maximum conditions, we have the following expression for the threshold energy E^{II}_{th} of Mechanism 2:

$$E^{II}_{th} = \frac{E_B}{\gamma_{13}} \frac{(1 + \mu_{12})^{2m+4}}{(1+\mu_{12}\cos\phi_1)^4 (1+2\mu_{12}\cos\phi_1+\mu_{12}^2)^m}, \qquad (20)$$

where ϕ_1 is the solution of the following transcendental equation:

$$2\theta_b + (m+2)\theta_a = \pi - \theta_0 . \qquad (21)$$

Only for m = 0 the above transcendental equation can be solved analytically, i.e., $\phi_1 = (\pi - \theta_0)/2$, where m = 0 means the three-collision-desorption process.

Mechanism 2 is in a sense the inverse process of Mechanism 1. Therefore, the expression of the threshold energy should have the similar form. With the help of Eq. (19) Eq. (20) can be written in the form

$$E^{II}_{th} = \frac{E_B}{\gamma_{13}} \frac{1}{\cos^4\theta_b} \left(\frac{1+\mu_{12}}{\cos\theta_b + (\mu_{12}^2 - \sin^2\theta_b)^{1/2}} \right)^{2m+4} . \qquad (22)$$

This expression is completely the same as that of Eq. (13) if one replace μ_{12} by μ_{32}, and θ_b is the solution of the equation

$$2\theta_b + (m+2)\arccos \frac{(\mu_{12}^2 - \sin^2\theta_b)^{1/2}}{\mu_{12}} = \pi - \theta_0, \qquad (23)$$

and similarly to Mechanism 1 we have the following approximate formula

$$\tilde{E}^{II}_{th} = \frac{E_B}{\gamma_{13}} \frac{1}{\cos^4(\tau_{12,m}\mu_{12})} \times \left(\frac{1+\mu_{12}}{\cos(\tau_{12,m}\mu_{12}) + \mu_{12}\cos(\tau_{12,m})} \right)^{2m+4} . \qquad (24)$$

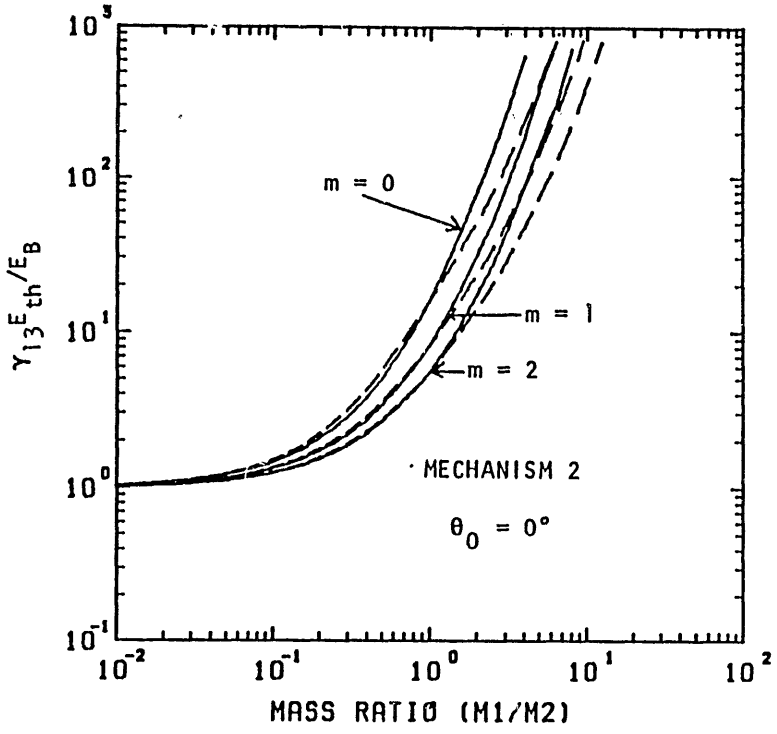

Fig. 6 Comparison of the exact threshold energies E^{II}_{th} with the approximate ones $\tilde{E}^{II}_{th}$ which are calculated from Eq. (24), where the angle of incidence is normal, and m is the collision number inside the substrate material. The solid lines and the broken lines correspond to E^{II}_{th} and $\tilde{E}^{II}_{th}$, respectively.

In Fig. 6. the m-dependences of threshold energies of Mechanism 2 are shown as a function of μ_{12} for the normal incidence, where the approximate threshold energies are also drawn in broken lines. The μ_{12} -dependences and the m-dependences of E^{II}_{th} are completely the same as those of E^{I}_{th} which are shown in Fig. 4.

2.3 Mechanism 3

Mechanism 3 means the sputtered-atom contribution, and the outward flux of sputtered substrate atoms knock off adsorbate atoms on their way out. Therefore, Mechanism 3 is the same mechanism as the near-threshold

mechanism of sputtering. Then Mechanism 3 can be divided into two patterns, i.e., Mechanism 3A and Mechanism 3B.

In the case of the Mechanism 3A the projectile after the first collision makes several scatterings with substrate atoms, and finally knocks off the substrate atom near the surface. This sputtered atom hits the adsorbate atom at the outermost layer. This mechanism is important for the case where the the atomic mass of the projectile is smaller than that of the substrate atom (see Fig. 7).

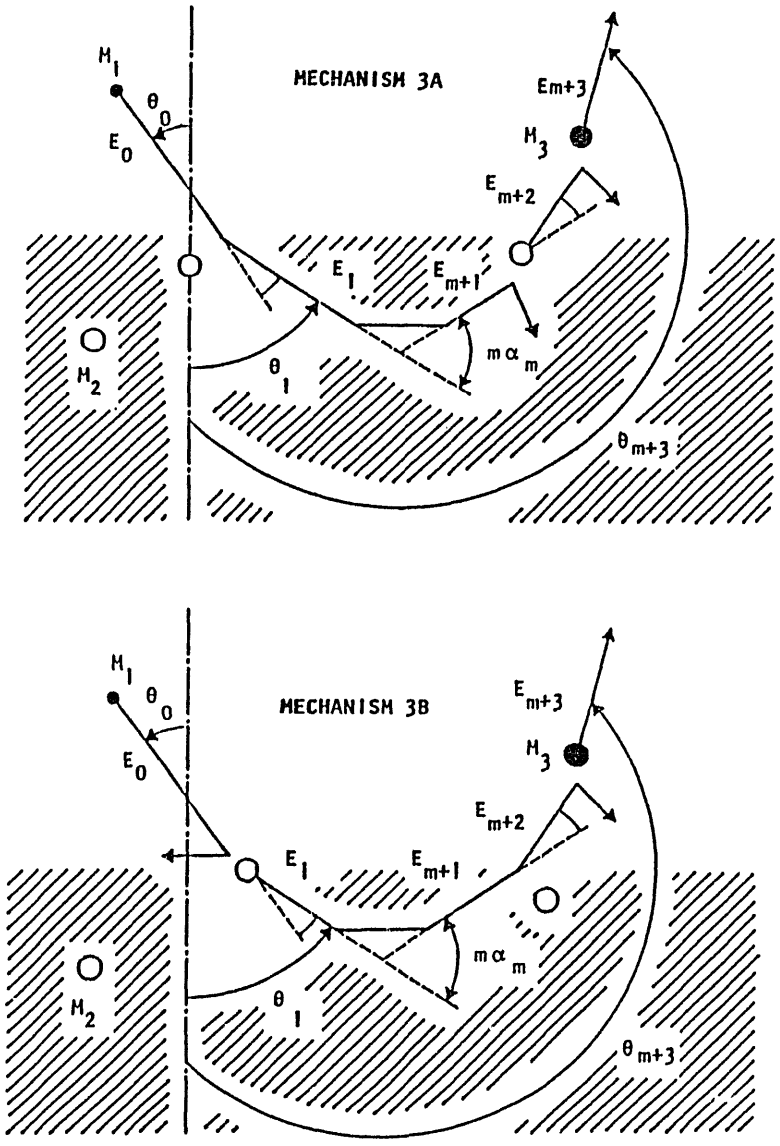

Fig. 7 Schematic representation of ion-induced desorption of Mechanism 3A and 3B.

In th case of Mechanism 3B, the primary recoil atom is produced at the first collision. After several equal-mass collisions, the primary recoil atom kicks off the adsorbed atom at the topmost layer (see Fig. 7). During a sequence of equal mass collisions the second or higher recoil atom will be produced, but from the viewpoint of threshold energy the higher-order recoil atom can be regarded as the scattering of the primary recoil atom [2].

First of all let us discuss Mechanism 3A. As is shown in the upper column of Fig. 7, after the first collision the projectile with energy E_1 is assumed to make the m equal-angle collisions with the substrate atoms. The vertical component E^A_+ of the energy E_{m+3} of the outgoing adsorbate atom is given as

$$E^A_+ = E_0 \gamma_{12}\gamma_{23}\,(1-\gamma_{12}\sin^2\frac{\phi_1}{2})(1-\gamma_{12}\sin^2\frac{\beta_m}{2})^m$$

$$\times \sin^2\frac{\phi_2}{2}\sin^2\frac{\phi_3}{2}\cos^2(\theta_0+\theta_a+m\alpha_m-\frac{\phi_2+\phi_3}{2}), \quad (25)$$

Where ϕ_2 and ϕ_3 are the CM scattering angles of the (m + 2)th- and the (m + 3)th- collisions, respectively. This expression is the same as that of Mechanism 2C of sputtering thresholds of Ref. 2 except for the additional term γ_{23}.

Differentiations with respect to ϕ_3, ϕ_2, β_m, ϕ_1 yield the following expression for the threshold energy E^A_{th} of Mechanism 3A:

$$E^A_{th} = \frac{E_B}{\gamma_{12}\gamma_{23}}\,\frac{(1+\mu_{12})^{2m+2}(1+2\mu_{12}\cos\phi_1+\mu_{12}^2)^{2-m}}{(1+\mu_{12}\cos\phi_1)^6}, \quad (26)$$

or

$$E^A_{th} = \frac{E_B}{\gamma_{12}\gamma_{23}}\,\frac{1}{\cos^6\theta_b}\left[\frac{1+\mu_{12}}{\cos\theta_b+(\mu_{12}^2-\sin^2\theta_b)^{1/2}}\right]^{2m+2}, \quad (27)$$

where ϕ_1 and θ_a are the solutions of the following transcendental equations:

$$3\theta_b + (m+1)\theta_a = \pi - \theta_0 \ , \tag{28}$$

$$3\theta_b + (m+1)\arccos\frac{(\mu_{12}^2 - \sin^2\theta_b)^{1/2}}{\mu_{12}} = \pi - \theta_0 \ , \tag{29}$$

Here, θ_a and θ_b of Eq. (28) are functions of ϕ_1 of which explicit expression are given by Eqs. (18) and (19), and the approximate formula for $E^A{}_{th}$ is easily obtained in a similar manner:

$$\tilde{E}^A{}_{th} = \frac{E_B}{\gamma_{12}\gamma_{23}}\frac{1}{\cos^6(\tau_{12,m}\mu_{12})} \times \left[\frac{1+\mu_{12}}{\cos(\tau_{12,m}\mu_{12})+\mu_{12}\cos(\tau_{12,m})}\right]^{2m+2} . \tag{30}$$

For Mechanism 3B the vertical component $E^B{}_+$ of E_{m+3} is as follows:

$$E^B{}_+ = E_0\gamma_{12}\gamma_{23}\sin^2\frac{\phi_1}{2}\cos^{2m}\frac{\beta_m}{2}\sin^2\frac{\phi_3}{2} \times \cos^2\left(\theta_0 - \frac{\phi_1 - m\beta_m + \phi_3}{2}\right), \tag{31}$$

where use is made of $\alpha_m = \beta_m/2$ because of the equal-mass collision. This expression has the same form as that of the sputtering mechanism Mechanism 1 of Ref. 2 except for the additional term γ_{23}.

Then we have very simple formula for Mechanism 3B as follows:

$$E^{B}_{th} = \frac{E_B}{\gamma_{12}\gamma_{23}} \frac{1}{\sin^{2m+8}\dfrac{(m+2)\pi + 2\theta_0}{2m+8}} . \qquad (32)$$

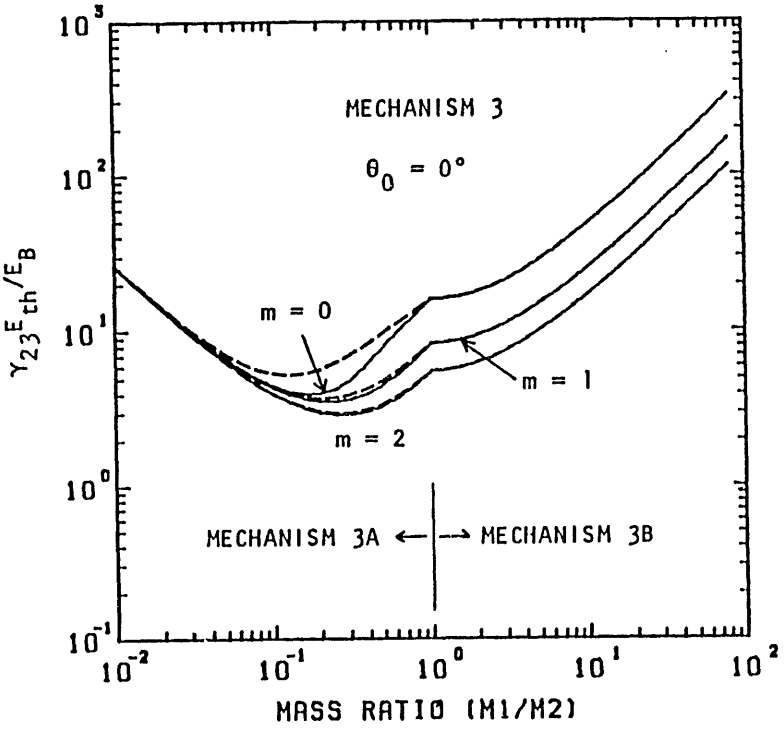

Fig. 8 Threshold energies of Mechanism 3 and comparison of the exact ones E^{A}_{th} (solid lines) with the approximate ones $\tilde{E}^{A}_{th}$ (broken lines) which are calculated from Eq. (32), where the angle of incidence is normal, and m is the collision number inside the substrate.

In Fig. 8 the threshold energies of Mechanism 3 are plotted as a function of mass ratio μ_{12} for different values m. The threshold mechanism for $\mu_{12} < 1$ is Mechanism 3A, while that for $\mu_{12} > 1$ Mechanism 3B. This mass-ratio dependence of $\gamma_{23}E_{th}/E_B$ is coincident with the relative threshold energy of the sputtering yield. The present approximate formula E^{A}_{th} is very good for m = 1 or m = 2.

The ion-induced desorption thresholds derived in Sections 2.1, 2.2, and 2.3 are based on the assumption that the adsorbate atoms are completely

isolated. When the adsorbate layer is enough thick, the threshold energies of Mechanism 1 become equal to those of Mechanism 3B, while Mechanism 2 is equivalent to Mechanism 3A because of $M_2 = M_3$. Therefore, threshold energies of the ion-induced desorption should show the same mass-ratio dependence as those of sputtering thresholds.

III. RESULTS AND DISCUSSIONS

In the previous chapter the general formulae for threshold energies of different desorption mechanisms were derived based on the binary collision approximation, where we assumed that any configuration of adsorbate atoms and substrate atoms was allowed for the threshold mechanism and that the adsorbed atom were completely isolated from each other. Every formula includes the unknown parameter m which is the collision number inside the substrate. This collision number can be regarded as the effective collision number when one uses the binary collision approximation for the successive collisions of very low-energy ion.

Up to now there is no measured data on ion-induced desorptions for the near threshold energy ions. Recent works on sputtering thresholds tell us that m = 1 or m = 2 is reasonable for the estimation of sputtering thresholds, and, then, m = 2 was used in Ref. 2. Let us use again m = 2 for the desorption threshold. In Table 1 the explicit expressions for the threshold energy of each mechanism are shown.

From Table 1 we can abstract the following properties of the relative threshold energy $\xi_{th} = E_{th}/E_b$ at the normal incidence:

1) When μ_{32} is less than μ_{12}, ξ^{I}_{th} has the lower values than ξ^{II}_{th}, and vice versa, because ξ^{I}_{th} is an increasing function of μ_{32}.

2) When μ_{12} is less than unity, Mechanism 3A is responsible for the threshold mechanism only for $M_1 < M_2 < M_3$ where $\gamma_{12}\gamma_{23} > \gamma_{13}$ and $\mu_{12} < \mu_{32}$.

Table 1 Theoretical formulae of the ion-induced desorption thresholds for different mechanisms.

Mechanisms	Formula
Mechanism 1[a]	$\frac{E_B}{\gamma_{13}} \frac{1}{\cos^4\theta} \left[\frac{1+\mu_{32}}{\cos\theta + (\mu_{32}^2 - \sin^2\theta)^{1/2}} \right]^8$
Mechanism 2[b]	$\frac{E_B}{\gamma_{13}} \frac{1}{\cos^4\theta_b} \left[\frac{1+\mu_{12}}{\cos\theta_b + (\mu_{12}^2 - \sin^2\theta_b)^{1/2}} \right]^8$
Mechanism 3A	$\frac{E_B}{\gamma_{12}\gamma_{23}} \left[\frac{1+\mu_{12}}{1+\mu_{12}\cos((\pi-\theta_0)/3)} \right]^6$
Mechanism 3B	$\frac{E_B}{\gamma_{12}\gamma_{23}} \frac{1}{\sin^{12}\{(2\pi+\theta_0)/6\}}$

[a] θ is the solution of the transcendental equation

$$2\theta + 4 \arccos \frac{(\mu_{32}^2 - \sin^2\theta)^{1/2}}{\mu_{32}} = \pi - \theta_0 .$$

[b] θ_b is the solution of the transcendental equation

$$2\theta_b + 4 \arccos \frac{(\mu_{12}^2 - \sin^2\theta_b)^{1/2}}{\mu_{12}} = \pi - \theta_0$$

3) For $M_2 = M_3$, ξ^{I}_{th} is equal to ξ^{B}_{th}, and for $M_1 = M_2$, ξ^{II}_{th} and ξ^{A}_{th} are equal to ξ^{B}_{th}.

4) For the finite value of μ_{23}, ξ^{A}_{th} has the minimum value at $\mu_{12} = 0.275$.

5) The relative threshold energy ξ^{B}_{th} has the minimum value at $M_2 = \sqrt{M_1 M_2}$.

In the desorption process we have to treat three different ion-target combinations. Moreocer, it is very difficult to discuss the threshold energies by some simple scaling rule. In the following sections the projectile (M_1) dependence, the substrate (M_2) dependence, the adsorbate (M_3) dependence, and the bombarding-angle (θ_0) dependence of desorption thresholds will be discussed one by one.

3.1 The projectile dependence of threshold energies at normal incidence

In Fig. 9, 10 and 11 the relative threshold energies E_{th}/E_B at normal incidence are plotted against the atomic mass (M_1) of the projectile for H on W, S on Ni, and S on Si which correspond to the cases of $\mu_{32} \ll 1$, $\mu_{32} < 1$, and $\mu_{32} > 1$, respectively

In the case of H on W (Fig. 9) the threshold energy of light-ion is nearly equal to unity, and the threshold mechanism is Mechanism 1 for any projectile because the condition of $\mu_{32} < \mu_{12}$ is satisfied for all projectiles. The M_1 dependence of this case is given as

$$\frac{E_{th}}{E_B} = \frac{1}{\gamma_{31}} \left[\frac{1 + \mu_{32}}{1 + \mu_{32}/\sqrt{2}} \right]^8 . \qquad (33)$$

Since γ_{31} is a decreasing function of M_1, the relative threshold energy is an increasing function of M_1.

In the case of S on Ni (Fig. 10) Mechanism 2 is responsible for the threshold mechanism until $M_1 = 32$ which is equal to the atomic mass of

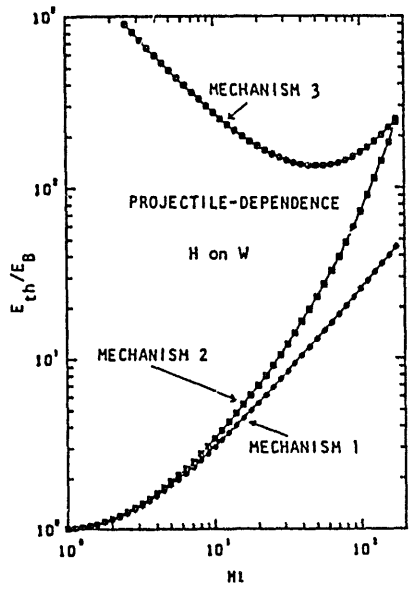

Fig. 9 The M_1-dependences of threshold energies of various desorption mechanisms for H on W, where θ_0=0.

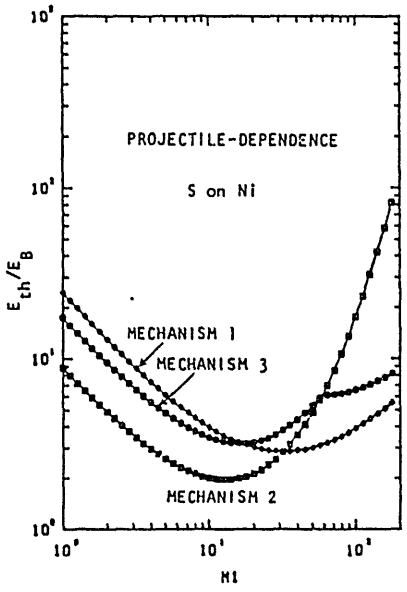

Fig. 10 The same as Fig. 9, but for S on Ni.

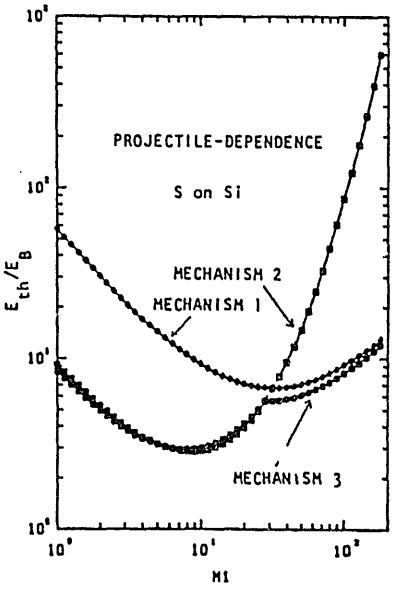

Fig. 11 The same as Fig. 9, but for S on Si.

the adsorbate S. In the region of $M_1 < 32$, $\mu_{12} < 1$, $\mu_{32} > 1$, and M_3 is less than M_2. This is why the threshold mechanism is Mechanism 1 is Mechanism 2. For $M_1 > 32$ the mass ratio μ_{32} is less than unity, and so Mechanism 1 is responsible for the threshold mechanism. The M_1 dependence of this case is reasonably predicted by the approximate formula of Eqs. (24) and (15).

In the case of S on Si (Fig. 11) the atomic masses of S and Si are nearly equal, and so the threshold energies of this system is roughly equal to those of Mechanism 3. When the adsorbate layer is thick, the atomic mass of adsorbate atom is equal to that of the substrate atom. This means that the difference between Mechanism 1 and Mechanism 3B disappears and that Mechanism 2 is equivalent to Mechanism 3A. Therefore, the

M_1-dependence of this case is given as

$$\frac{E_{th}}{E_B} = \begin{cases} \dfrac{1}{\gamma_{12}\gamma_{23}} \left\{ \dfrac{2 + 2\mu_{12}}{2 + \mu_{12}} \right\}^6 & M_1 < 28 \\ \dfrac{1}{\gamma_{12}\gamma_{23}} \left(\dfrac{4}{3} \right)^6 & M_1 > 28. \end{cases} \tag{34}$$

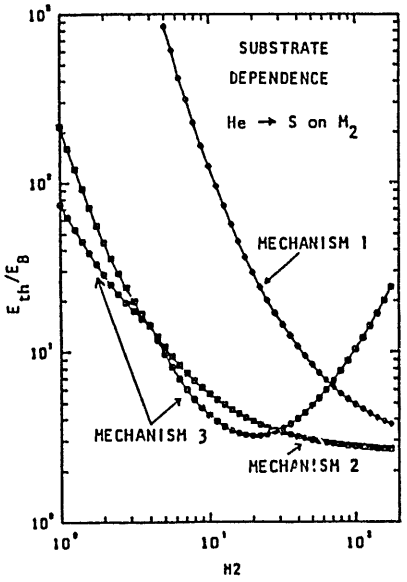

Fig. 12 The M_2-dependences of threshold energies of various desorption mechanisms for He→S on M_2, where $\theta_0 = 0$.

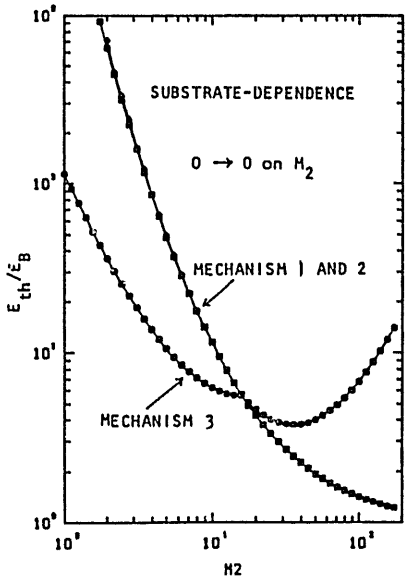

Fig. 13 The same as Fig.12, but for O→O on M_2.

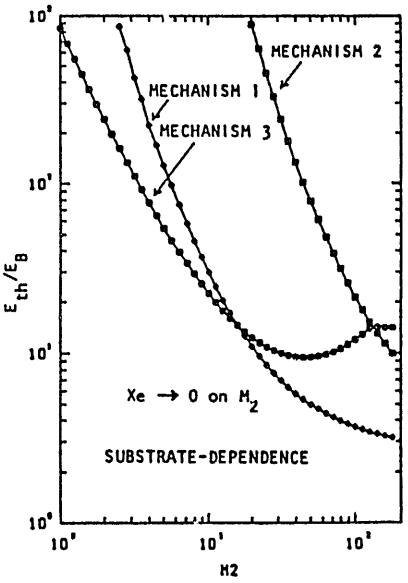

Fig. 14 The same as Fig. 12, but for Xe→O on M_2.

3.2 The substrate dependence of threshold energies at normal incidence

In Figs. 12, 13 and 14 the relative threshold energies E_{th}/E_B at normal incidence are plotted as a function of the atomic mass (M_2) of the substrate atom for three different projectile-substrate combinations, i.e., He-S, O-O, and Xe-O. These three combinations corresponds to the case of $\mu_{13} < 1$, $\mu_{13} = 1$, and $\mu_{13} > 1$, respectively.

In the case of He-S (Fig. 12) Mechanism 3B is the threshold mechanism for $M_2 < 4$ where $\mu_{12} > 1$ and $\mu_{32} > 1$. For $M_2 > 4$ the mass ratio μ_{12} is less than unity and so there is the possibility that Mechanism 3A or Mechanism 2 becomes the threshold mechanism. In the region of $4 < M_2 < 32$, $\gamma_{12}\gamma_{23}$ is larger than γ_{13} and so Mechanism 3A is responsible for the threshold mechanism. For $M_2 > 32$ Mechanism 2 is the threshold mechanism and the condition of $\mu_{32} << 1$ is satisfied. Then the M_2 dependence of the region of $M_2 > 32$ is roughly expressed as

$$\frac{E_{th}}{E_B} = \frac{1}{\gamma_{13}}\left(\frac{1+\mu_{12}}{1+\mu_{12}/\sqrt{2}}\right)^8 . \qquad (35)$$

In the case of O-O (Fig. 13) the threshold energy of Mechanism 1 is equal to that of Mechanism 2. Until $M_2 = 16$ the mass ratio μ_{12} is larger than unity and so Mechanism 3B is responsibel for the threshold mechanism. From Figs. 12 and 13 we know that for $\mu_{12} > 1$ Mechanism 3B is always the threshold mechanism. Since $\mu_{12} < 1$ and $M_2 > M_3$ for $M_2 > 16$, the threshold mechanism is Mechanism 1 or 2 and the M_2 dependence is well described by Eq. (15).

In the case of Xe-O (Fig. 14) the mass ratios μ_{12} and μ_{32} are larger than unity until $M_2 = 16$ and so the threshold mechanism 3B. The threshold-energy curve of Mechanism 3B has the minimum value at $M_2 = 58.7$ which corresponds to $\sqrt{M_1 M_2}$. For $M_2 > 16$ the mass ratio μ_{32} is less than unity and so Mechanism 1 becomes the threshold mechanism.

3.3 Adsorbate dependence of threshold energies at normal incidence

In Figs. 15, 16 and 17 the relative threshold energies E_{th}/E_B at normal incidence are plotted against the atomic mass (M_3) of the adsorbate atom for three different projectile-substrate combinations, i.e., H+Ni, Ar+W and Xe+Ni. These three combinations correspond to the case of $\mu_{12} << 1$,

$\mu_{12} < 1$ and $\mu_{12} > 1$, respectively.

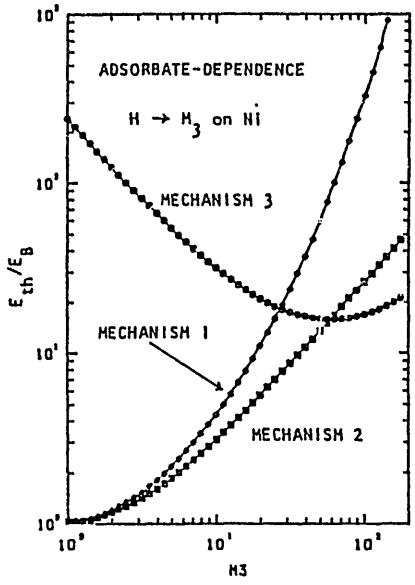

Fig. 15 The M_3-dependences of threshold energies of various desorption mechanisms for $H \rightarrow M_3$ on Ni, where $\theta_0 = 0$.

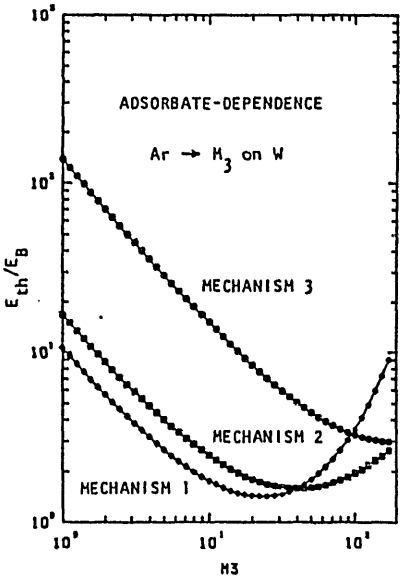

Fig. 16 The same as Fig. 15, but for $Ar \rightarrow M_3$ on W.

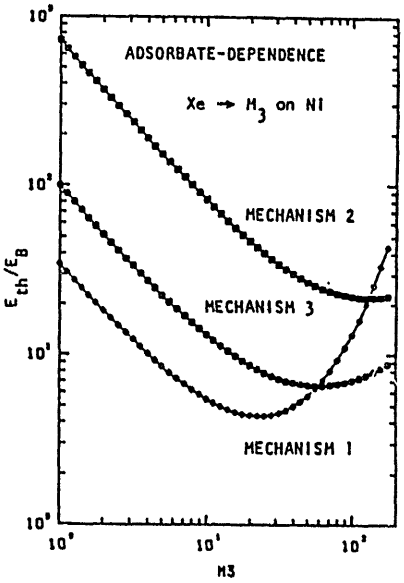

Fig. 17 The same as Fig. 15, but for $Xe \rightarrow M_3$ on Ni.

In the case of H+Ni (Fig. 15) the threshold mechanism is Mechanism 2 until $M_3 = 58.7$ where the condition of $\mu_{12} << \mu_{32} < 1$ is satisfied. When M_2 becomes larger than 58.7 the inequality $M_1 < M_2 < M_3$ is held and so the threshold mechanism is Mechanism 3A. For $\mu_{12} << 1$ the M_3 dependence of Mechanism 2 is represented by Eq. (35), and that of Mechanism 3A is given by the upper formula of Eq. (34). AS the threshold-energy formula of Mechanism 3A for $\mu_{12} << 1$, we have the following expression [6]:

$$\frac{E_{th}}{E_B} = \frac{1}{\gamma_{12}\gamma_{23}(1 - \gamma_{12})}, \qquad (36)$$

which can be easily derived from Eq. (30) if one set m = 0 under the condition of $\mu_{12} \ll 1$.

In the case of Ar+W (Fig. 16) Mechanism 1 is the threshold mechanism until M_3 = 39.35 where the inequality $\mu_{32} < \mu_{12} < 1$ is satisfied. In the region of $39.5 < M_2 < 183.9$ the condition of $\mu_{12} < \mu_{32} < 1$ is satisfied and so Mechanism 2 is the threshold mechanism.

In the case of Xe+Ni (Fig. 17) Mechanism 1 is the threshold mechanism until M_3 = 58.7, because of $\mu_{32} < 1$ and $\mu_{12} > 1$. When M_3 is larger than 58.7 Mechanism 3B is threshold mechanism of which curve has the minimum value at M_3 = 58.7.

From Figs. 9 through 17 we know that Mechanism 1 can not be responsible the threshold mechanism for $\mu_{32} > 1$ and Mechanism 2 does not becomes the threshold mechanism for $\mu_{12} < 1$. In Table 2 we summarize possible combinations of the projectile, substrate and adsorbate, and the corresponding threshold mechanism, and the corresponding analytical formula at not-too-oblique incidence.

3.4 The bombarding-angle dependence of threshold energies

As is known from Table 2 each analytical formula has different bombarding-angle dependence. The bombarding-angle dependence of the threshold energy of Mechanism 3B is the strongest among the present formulae and so even if Mechanism 3B is not the threshold mechanism at small angles of incidence there is the possibility that Mechanism 3B will become responsible for the threshold mechanism at large angles of incidence.

When the angle of incidence becomes large, we should take into account the shadowing effect and the effective periodicity of surface atoms except for Mechanism 1 [2]. At present the binding energy of the adsorbate atom is not well established for any adsorbate substrate combination. Therefore it is very difficult to estimate the shadowing effects

Table 2 Analytical formulae of ion-induced desorption thresholds for possible combinations of the projectile, the substrate and the adsorbate

Combinations	Threshold mechanism	Formula
$M_1 < M_2 < M_3$	Mechanism 3A	$\frac{E_B}{\gamma_{12}\gamma_{23}}\left[\frac{1+\mu_{12}}{1+\mu_{12}\cos\{(\pi-\theta_0)/3\}}\right]^6$
$M_1 < M_3 < M_2$	Mechanism 2	$\frac{E_B}{\gamma_{13}}\frac{1}{\cos^4\{\frac{(\pi-\theta_0)\mu_{12}}{4+2\mu_{12}}\}}\left[\frac{1+\mu_{12}}{\cos\{\frac{(\pi-\theta_0)\mu_{12}}{4+2\mu_{12}}\}+\mu_{12}\cos\frac{\pi-\theta_0}{4+2\mu_{12}}}\right]^8$
$M_2 < M_1 < M_3$ $M_2 < M_3 < M_1$	Mechanism 3B	$\frac{E_B}{\gamma_{12}\gamma_{23}}\frac{1}{\sin^{12}\frac{2\pi+\theta_0}{6}}$
$M_3 < M_1 < M_2$ $M_3 < M_2 < M_1$	Mechanism 1	$\frac{E_B}{\gamma_{13}}\frac{1}{\cos^4\{\frac{(\pi-\theta_0)\mu_{32}}{4+2\mu_{32}}\}}\left[\frac{1+\mu_{32}}{\cos\{\frac{(\pi-\theta_0)\mu_{32}}{4+2\mu_{32}}\}+\mu_{32}\cos\frac{\pi-\theta_0}{4+2\mu_{32}}}\right]^8$

reasonably and so in this paper this effect is not considered. In Figs. 18 through 23 the bombarding-angle dependences of threshold energies of four mechanisms are shown for possible mechanisms listed in Table 2, i.e.,

1) Fig. 18 : $M_1 < M_2 < M_3$ (He → S on Si)
2) Fig. 19 : $M_1 < M_3 < M_2$ (H → S on Ni)
3) Fig. 20 : $M_2 < M_1 < M_3$ (Si → S on Al)
4) Fig. 21 : $M_2 < M_3 < M_1$ (Ar → S on Si)
5) Fig. 22 : $M_3 < M_1 < M_2$ (Ar → S on W)
6) Fig. 23 : $M_3 < M_2 < M_1$ (Xe → S on Ni)

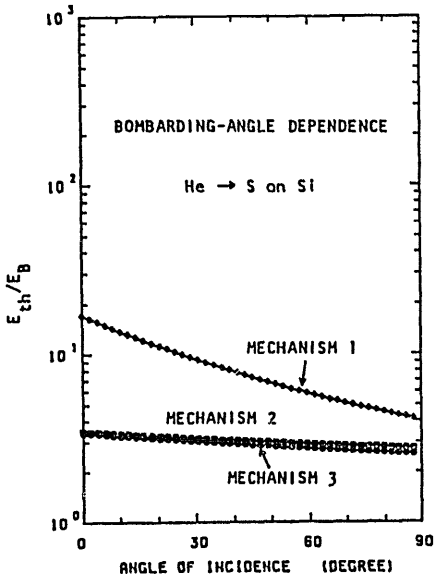

Fig. 18 The θ_0-dependences of threshold energies of various desorption mechanisms for He→S on Si.

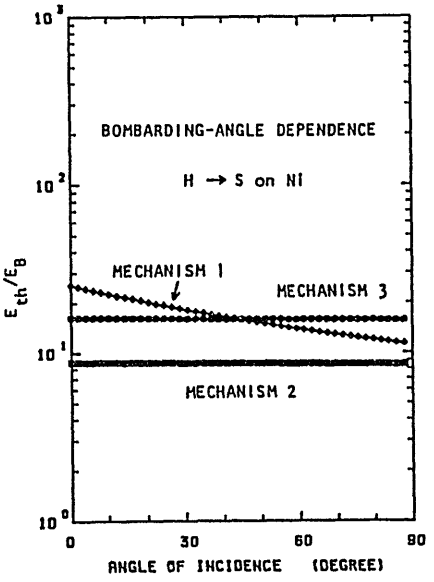

Fig. 19 The same as Fig. 18, but for H→S on Ni.

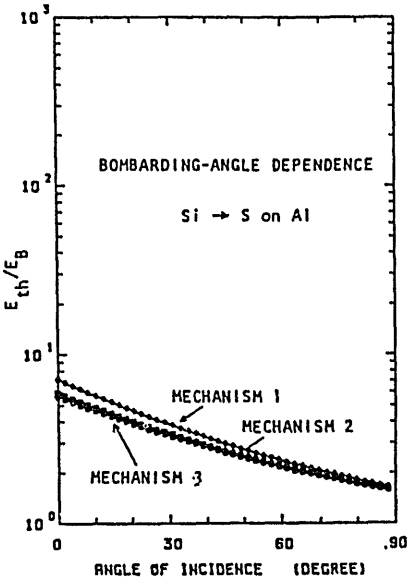

Fig. 20 The same as Fig. 18, but for Si→S on Al.

The threshold mechanisms of these six combinations at small angle of incidence are Mechanism 3A, Mechanism 2, Mechanism 3B, Mechanism 3B, Mechanism 1, and Mechanism 1, respectively, which are coincident with the threshold mechanisms of Table 2.

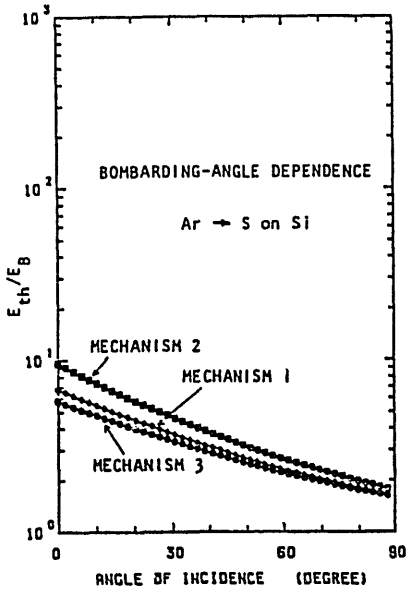

Fig. 21 The same as Fig. 18 but for Ar→S on Si.

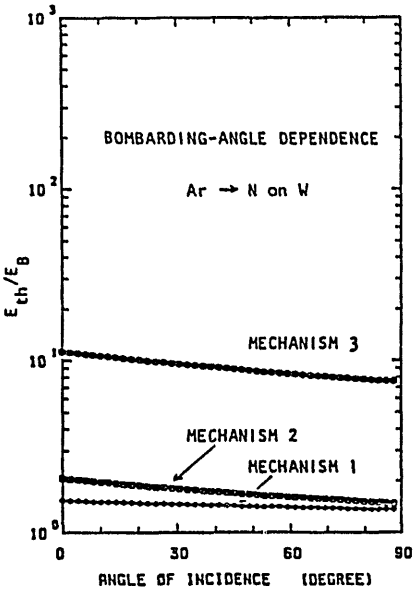

Fig. 22 The same as Fig. 18, but for Ar→N on W.

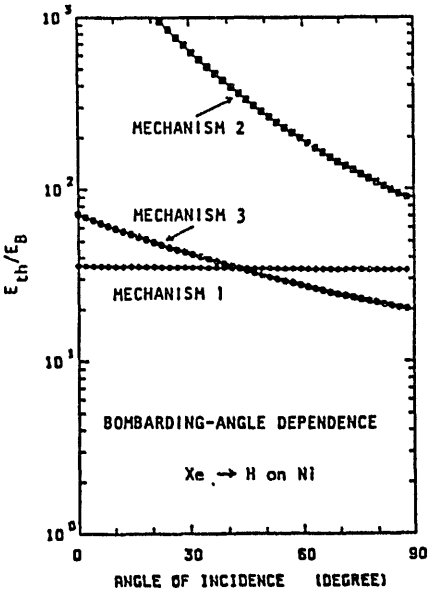

Fig. 23 The same as Fig. 18, but for Xe→H on Ni.

Except for Fig. 23 the threshold mechanism does not change in the whole region of θ_0. In the case of $M_3 < M_2 < M_1$ the mass ratio μ_{12} is larger than unity and so E^B_{th} has the second minimum value. This is why Mechanism 3B is responsible for the threshold mechanism for larger angles of incidence.

IV. CONCLUSIONS

Assuming the random configuration of the adsorbate atom and the substrate atom, analytic formulae of the ion-induced desorption thresholds have been derived for various combinations of the projectile, the substrate atom, and the adsorbate atom, where we adopted the isolated-adsorbate-atom model.

The threshold mechanism corresponds to the minimum energy-loss process. The minimum energy-loss condition says that the particle with the smallest

mass among the projectile, the substrate atom and the adsorbate atom should move in solids.

Within the present model of the isolated adsorbate atoms, it is found that the combinations of the projectile, the substrate atom, and the adsorbate atom can be classified into four categories, i.e.,

1) $M_1 < M_2 < M_3$, 2) $M_1 < M_3 < M_2$,

3) $M_2 < M_1, M_3$, 4) $M_3 < M_1, M_2$,

where M_1, M_2, and M_3 are the atomic masses of the projectile, the substrate atom, and the adsorbate atom, respectively. These four categories have different analytic formulae of ion-induced desorption thresholds.

In the case of the third category mentioned above, the threshold energy is a decreasing function of the angle of incidence, meanwhile the threshold energies of other three cases do not depend on the angle of incidence so strongly.

ACKNOWLEDGMENTS

We(Y.Y) would like to thank W. Eckstein, J. Roth, H. Verbeek, and B.M.U. Scherzer for many valuable discussions.

REFERENCES

1) S.M. Liu, W.E. Rodgers, and E.L. Knuth, J. Chem. Phys. 61 (1974) 50.

2) Y. Yamamura and J. Bohdansky, Vacuum 35 (1985) 561.

3) Y. Yamamura and Y. Mizuno, J.Nucl. Mater. 128&129 (1984) 559.

4) E. Eckstein, private communications.

5) H.F. Winters and P. Sigmund,J. Appl. Phys.45 (1974) 4760.

6) E. Taglauer, Data Compendium for Plasma-Surface Interactions , in Nucl. Fusion Special Supplement, International Atomic Energy Agency, Vienna (1984) p.43.

LIST OF IPPJ-AM REPORTS

IPPJ-AM-1* "Cross Sections for Charge Transfer of Hydrogen Beams in Gases and Vapors in the Energy Range 10 eV–10 keV"
H. Tawara (1977) [Published in Atomic Data and Nuclear Data Tables 22, 491 (1978)]

IPPJ-AM-2* "Ionization and Excitation of Ions by Electron Impact –Review of Empirical Formulae–"
T. Kato (1977)

IPPJ-AM-3 "Grotrian Diagrams of Highly Ionized Iron FeVIII-FeXXVI"
K. Mori, M. Otsuka and T. Kato (1977) [Published in Atomic Data and Nuclear Data Tables 23, 196 (1979)]

IPPJ-AM-4 "Atomic Processes in Hot Plasmas and X-Ray Emission"
T. Kato (1978)

IPPJ-AM-5* "Charge Transfer between a Proton and a Heavy Metal Atom"
S. Hiraide, Y. Kigoshi and M. Matsuzawa (1978)

IPPJ-AM-6* "Free-Free Transition in a Plasma –Review of Cross Sections and Spectra–"
T. Kato and H. Narumi (1978)

IPPJ-AM-7* "Bibliography on Electron Collisions with Atomic Positive Ions: 1940 Through 1977"
K. Takayanagi and T. Iwai (1978)

IPPJ-AM-8 "Semi-Empirical Cross Sections and Rate Coefficients for Excitation and Ionization by Electron Collision and Photoionization of Helium"
T. Fujimoto (1978)

IPPJ-AM-9 "Charge Changing Cross Sections for Heavy-Particle Collisions in the Energy Range from 0.1 eV to 10 MeV I. Incidence of He, Li, Be, B and Their Ions"
Kazuhiko Okuno (1978)

IPPJ-AM-10 "Charge Changing Cross Sections for Heavy-Particle Collisions in the Energy Range from 0.1 eV to 10 MeV II. Incidence of C, N, O and Their Ions"
Kazuhiko Okuno (1978)

IPPJ-AM-11 "Charge Changing Cross Sections for Heavy-Particle Collisions in the Energy Range from 0.1 eV to 10 MeV III. Incidence of F, Ne, Na and Their Ions"
Kazuhiko Okuno (1978)

IPPJ-AM-12* "Electron Impact Excitation of Positive Ions Calculated in the Coulomb-Born Approximation –A Data List and Comparative Survey–"
S. Nakazaki and T. Hashino (1979)

IPPJ-AM-13 "Atomic Processes in Fusion Plasmas – Proceedings of the Nagoya Seminar on Atomic Processes in Fusion Plasmas Sept. 5-7, 1979"
Ed. by Y. Itikawa and T. Kato (1979)

IPPJ-AM-14 "Energy Dependence of Sputtering Yields of Monatomic Solids"
N. Matsunami, Y. Yamamura, Y. Itikawa, N. Itoh, Y. Kazumata, S. Miyagawa, K. Morita and R. Shimizu (1980)

IPPJ-AM-15 "Cross Sections for Charge Transfer Collisions Involving Hydrogen Atoms"
Y. Kaneko, T. Arikawa, Y. Itikawa, T. Iwai, T. Kato, M. Matsuzawa, Y. Nakai, K. Okubo, H. Ryufuku, H. Tawara and T. Watanabe (1980)

IPPJ-AM-16 "Two-Centre Coulomb Phaseshifts and Radial Functions"
H. Nakamura and H. Takagi (1980)

IPPJ-AM-17 "Empirical Formulas for Ionization Cross Section of Atomic Ions for Electron Collisions –Critical Review with Compilation of Experimental Data–"
Y. Itikawa and T. Kato (1981)

IPPJ-AM-18 "Data on the Backscattering Coefficients of Light Ions from Solids"
T. Tabata, R. Ito, Y. Itikawa, N. Itoh and K. Morita (1981) [Published in Atomic Data and Nuclear Data Tables 28, 493 (1983)]

IPPJ-AM-19 "Recommended Values of Transport Cross Sections for Elastic Collision and Total Collision Cross Section for Electrons in Atomic and Molecular Gases"
M. Hayashi (1981)

IPPJ-AM-20 "Electron Capture and Loss Cross Sections for Collisions between Heavy Ions and Hydrogen Molecules"
Y. Kaneko, Y. Itikawa, T. Iwai, T. Kato, Y. Nakai, K. Okuno and H. Tawara (1981)

IPPJ-AM-21 "Surface Data for Fusion Devices – Proceedings of the U.S–Japan Workshop on Surface Data Review Dec. 14-18, 1981"
Ed. by N. Itoh and E.W. Thomas (1982)

IPPJ-AM-22 "Desorption and Related Phenomena Relevant to Fusion Devices"
Ed. by A. Koma (1982)

IPPJ-AM-23 "Dielectronic Recombination of Hydrogenic Ions"
T. Fujimoto, T. Kato and Y. Nakamura (1982)

IPPJ-AM-24 "Bibliography on Electron Collisions with Atomic Positive Ions: 1978 Through 1982 (Supplement to IPPJ-AM-7)"
Y. Itikawa (1982) [Published in Atomic Data and Nuclear Data Tables 31, 215 (1984)]

IPPJ-AM-25 "Bibliography on Ionization and Charge Transfer Processes in Ion-Ion Collision"
H. Tawara (1983)

IPPJ-AM-26 "Angular Dependence of Sputtering Yields of Monatomic Solids"
Y. Yamamura, Y. Itikawa and N. Itoh (1983)

IPPJ-AM-27 "Recommended Data on Excitation of Carbon and Oxygen Ions by Electron Collisions"
Y. Itikawa, S. Hara, T. Kato, S. Nakazaki, M.S. Pindzola and D.H. Crandall (1983) [Published in Atomic Data and Nuclear Data Tables 33, 149 (1985)]

IPPJ-AM-28 "Electron Capture and Loss Cross Sections for Collisions Between Heavy Ions and Hydrogen Molecules (Up-dated version of IPPJ-AM-20)
H. Tawara, T. Kato and Y. Nakai (1983) [Published in Atomic Data and Nuclear Data Tables 32, 235 (1985)]

IPPJ-AM-29 "Bibliography on Atomic Processes in Hot Dense Plasmas"
T. Kato, J. Hama, T. Kagawa, S. Karashima, N. Miyanaga, H. Tawara, N. Yamaguchi, K. Yamamoto and K. Yonei (1983)

IPPJ-AM-30 "Cross Sections for Charge Transfers of Highly Ionized Ions in Hydrogen Atoms (Up-dated version of IPPJ-AM-15)"
H. Tawara, T. Kato and Y. Nakai (1983) [Published in Atomic Data and Nuclear Data Tables 32, 235 (1985)]

IPPJ-AM-31 "Atomic Processes in Hot Dense Plasmas"
T. Kagawa, T. Kato, T. Watanabe and S. Karashima (1983)

IPPJ-AM-32 "Energy Dependence of the Yields of Ion-Induced Sputtering of Monatomic Solids"
N. Matsunami, Y. Yamamura, Y. Itikawa, N. Itoh, Y. Kazumata, S. Miyagawa, K. Morita, R. Shimizu and H. Tawara (1983) [Published in Atomic Data and Nuclear Data Tables 31, 1 (1984)]

IPPJ-AM-33 "Proceedings on Symposium on Atomic Collision Data for Diagnostics and Modelling of Fusion Plasmas, Aug. 29 – 30, 1983"
Ed. by H. Tawara (1983)

IPPJ-AM-34 "Dependence of the Backscattering Coefficients of Light Ions upon Angle of Incidence"
T. Tabata, R. Ito, Y. Itikawa, N. Itoh, K. Morita and H. Tawara (1984)

IPPJ-AM-35 "Proceedings of Workshop on Synergistic Effects in Surface Phenomena Related to Plasma-Wall Interactions, May 21 – 23, 1984"
Ed. by N. Itoh, K. Kamada and H. Tawara (1984) [Published in Radiation Effects 89, 1 (1985)]

IPPJ-AM-36 "Equilibrium Charge State Distributions of Ions ($Z_1 \geqq 4$) after Passage through Foils – Compilation of Data after 1972"
K. Shima, T. Mikumo and H. Tawara (1985) [Published in Atomic Data and Nuclear Data Tables 34, 357 (1986)]

IPPJ-AM-37 "Ionization Cross Sections of Atoms and Ions by Electron Impact"
H. Tawara, T. Kato and M. Ohnishi (1985) [Published in Atomic Data and Nuclear Data Tables 36, 167 (1987)]

IPPJ-AM-38 "Rate Coefficients for the Electron-Impact Excitations of C-like Ions"
Y. Itikawa (1985)

IPPJ-AM-39 "Proceedings of the Japan-U.S. Workshop on Impurity and Particle Control, Theory and Modeling, Mar. 12 – 16, 1984"
Ed. by T. Kawamura (1985)

IPPJ-AM-40 "Low-Energy Sputterings with the Monte Carlo Program ACAT"
Y. Yamamura and Y. Mizuno (1985)

IPPJ-AM-41 "Data on the Backscattering Coefficients of Light Ions from Solids (a Revision)"
R. Ito, T. Tabata, N. Itoh, K. Morita, T. Kato and H. Tawara (1985)

IPPJ-AM-42 "Stopping Power Theories for Charged Particles in Inertial Confinement Fusion Plasmas (Emphasis on Hot and Dense Matters)"
S. Karashima, T. Watanabe, T. Kato and H. Tawara (1985)

IPPJ-AM-43 "The Collected Papers of Nice Project/IPP, Nagoya"
Ed. by H. Tawara (1985)

IPPJ-AM-44 "Tokamak Plasma Modelling and Atomic Processes"
Ed. by T. Kawamura (1986)

IPPJ-AM-45 Bibliography of Electron Transfer in Ion-Atom Collisions
H. Tawara, N. Shimakura, N. Toshima and T. Watanabe (1986)

IPPJ-AM-46 "Atomic Data Involving Hydrogens Relevant to Edge Plasmas"
H. Tawara, Y. Itikawa, Y. Itoh, T. Kato, H. Nishimura, S. Ohtani, H. Takagi, K. Takayanagi and M. Yoshino (1986)

IPPJ-AM-47 "Resonance Effects in Electron-Ion Collisions"
Ed. by H. Tawara and G. H. Dunn (1986)

IPPJ-AM-48 "Dynamic Processes of Highly Charged Ions (Proceedings)"
Ed. by Y. Kanai and S. Ohtani (1986)

IPPJ-AM-49 "Wavelengths of K X-Rays of Iron Ions"
T. Kato, S. Morita and H. Tawara (1987)

IPPJ-AM-50 "Proceedings of the Japan-U.S. Workshop P-92 on Plasma Material Interaction/High Heat Flux Data Needs for the Next Step Ignition and Steady State Devices, Jan. 26 – 30, 1987"
Ed. by A. Miyahara and K. L. Wilson (1987)

IPPJ-AM-51 "High Heat Flux Experiments on C-C Composite Materials by Hydrogen Beam at the 10MW Neutral Beam Injection Test Stand of the IPP Nagoya"
H. Bolt, A. Miyahara, T. Kuroda, O. Kaneko, Y. Kubota, Y. Oka and K. Sakurai (1987)

IPPJ-AM-52 "Energy Dependence of Ion-Induced Sputtering Yields of Monatomic Solids in the Low Energy Region"
N. Matsunami, Y. Yamamura, N. Itoh, H. Tawara and T. Kawamura (1987)

IPPJ-AM-53 "Data Base on the High Heat Flux Behaviour of Metals and Carbon Materials for Plasma Facing Components – Experiments at the 10 MW Neutral Beam Injection Test Stand of the IPP Nagoya"
H. Bolt, C. D. Croessmann, A. Miyahara, T. Kuroda and Y. Oka (1987)

IPPJ-AM-54 "Final (n, ℓ) State-Resolved Electron Capture by Multiply Charged Ions from Neutral Atoms"
N. Shimakura, N. Toshima, T. Watanabe and H. Tawara (1987)

IPPJ-AM-55 "Atomic Data for Hydrogens in Collisions with Electrons – Addenda to IPPJ-AM-46"
H. Tawara, Y. Itikawa, H. Nishimura and M. Yoshino (1987)

IPPJ-AM-56 "Total and Partial Cross Sections for Electron Capture for C^{q+} (q= 6–2) and O^{q+} (q=8–2) Ions in Collisions with H, H_2 and He Atoms"
H. Tawara (1987)

IPPJ-AM-57 "Atomic Models for Hot Dense Plasmas"
K. Fujima (1988)

IPPJ-AM-58 "Recommended Data for Excitation Rate Coefficients of Helium Atoms and Helium-Like Ions by Electron Impact"
T. Kato and S. Nakazaki (1988)

IPPJ-AM-59 "Atomic and Molecular Processes in Edge Plasmas Including Hydrocarbon Molecules"
Ed. by H. Tawara (1988)

IPPJ-AM-60 "Theory of Threshold Energy of Ion-Induced Desorption by a Few-Collision Model"
Y. Yamamura, J. Bohdansky and E. Taglauer (1988)

Available upon request to Research Information Center, Institute of Plasma Physics, Nagoya University, Nagoya 464, Japan, except for the reports noted with*.